



5

10

Impacts of Differing Melt Regimes on Satellite Radar Waveforms and Elevation Retrievals

Alexander C. Ronan¹, Robert L. Hawley¹, Jonathan W. Chipman^{1,2}

15

¹Department of Earth Sciences, Dartmouth College, Hanover NH, 03755, United States

²Department of Geography, Dartmouth College, Hanover NH, 03755, United States

Correspondence to: Alexander C. Ronan (alexander.clark.ronan@dartmouth.edu)

20



25

Abstract. Geodetic surface mass balance calculations rely on satellite radar altimeters such as CryoSat-2 to understand elevation and volume changes of the Greenland Ice Sheet (GrIS). However, the impact of varying GrIS shallow subsurface stratigraphic conditions on Level 2 CryoSat-2 elevation products is poorly understood. We investigate the reliability of the Offset Center of Gravity (OCOG) and University College London Land-Ice elevation (ULI) retracking algorithms through the analysis of, and comparison with, Level 1B waveform-derived Leading-Edge Width (LeW). We generate a 2010 to 2021 LeW time series using temporal clustering and Bayesian Model averaging and compare with Level 2 OCOG and ULI elevation time series. This workflow is performed at Summit Station, NEEM, and Raven Camp, chosen to represent the upper and lower bounds of the dry-snow zone, and percolation zone respectively. We note that melting event, snowpack recovery, and potentially anomalous snow accumulation and high-speed winds signatures are evident in Summit Station's LeW time series. We find that Level 1B LeW has a significant inverse relationship with the ULI Level 2 elevations at NEEM and Summit Station, and likely the entire dry snow zone. The ULI Level 2 elevations at Raven Camp, and likely the entire percolation zone, have no clear elevation bias associated with significant melt events. The OCOG retracked elevations showed no significant association with LeW at any site. Future work is needed to understand the impacts of GrIS high-speed wind events and snow accumulation on elevation products, as well as to create retracking algorithms that are more resilient to abrupt changes in the shallow subsurface.

1. Introduction

The Greenland Ice Sheet (GrIS) contains 6-7 m of global sea-rise equivalent of ice (Cuffey & Marshall, 2000) and is predicted to contribute between 30-170 mm to sea-level rise by 2100 (Shepherd et al., 2019). GrIS elevation and mass balance products need to be as accurate as possible given its climatological significance in the face of warming temperatures. A valuable tool in developing such products is ESA's CryoSat-2 radar altimeter, SIRAL (European Space Agency, 2010). Unlike NASA's ICESat-2 laser elevation instrument ATLAS, SIRAL can penetrate the GrIS shallow subsurface (Neumann et al., 2019; Nilsson et al., 2015; Simonsen & Sørensen, 2017; Vermeer et al., 2022). CryoSat-2 elevation retrievals can be influenced by local and regional effects of surface melting and snowpack processes, as noted around NEEM from 2011 to 2014 (Nilsson et. al 2015). However, the impact of melt on radar waveforms and thus surface elevation retrievals is not uniform across the ice sheet.

As anthropogenic climate change accelerates the GrIS surface melt (Sellevoold & Vizcaíno, 2020) and increases interannual variability in surface mass balance (Fyke et al., 2014), melt-induced CryoSat-2- derived elevation biases are likely to remain significant. Therefore, the relationship between these elevation biases and changing shallow subsurface GrIS dynamics needs to be fully understood. Here, we analyze changes in the shallow subsurface and its influence on perceived retracked-derived

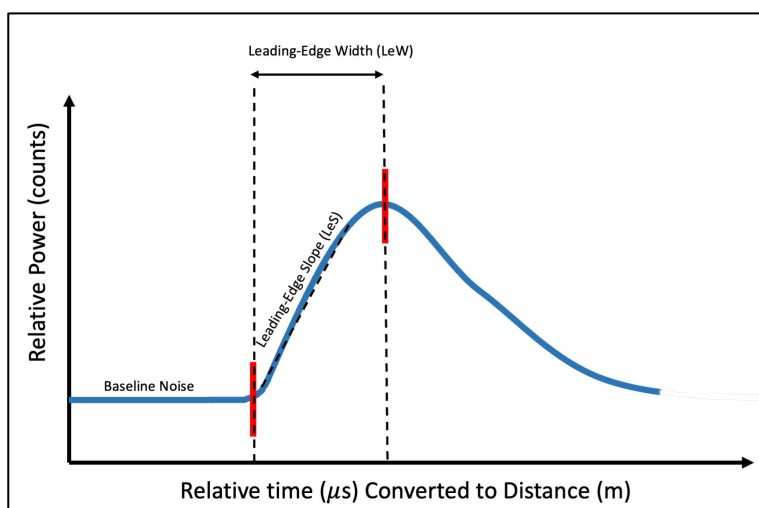


elevations from 2010-2021, and across locations dominated by different glaciological regimes in the dry-snow and percolation zones (Benson, 1996; Nghiem et al., 2001, 2012; Polashenski et al., 2014; Rizzoli et al., 2017).

2. Background

60 Researchers can choose from two supported retracking algorithms when analyzing SIRAL Level 2 Elevations across the contiguous Greenland Ice Sheet (GrIS): Offset Center of Gravity (OCOG) and UCL Land-Ice elevation (ULI). The ULI retracker fits incoming waveform data to a Brown - Hayne Model adapted to the CryoSat-2 instrument (European Space Agency, 2019), which assumes that the data are a convolution of a point target response, the effective area illuminated versus time, and the ocean surface roughness function (Garcia et al., 2014). The retracker then infers the location of the significant surface return through the slope of the waveform's leading edge (LeS) (Schlembach et al., 2020) (Figure 1). The LeS has an
65 inverse relationship with the waveform's Leading-edge width (LeW), assuming a constant amplitude (Figure 1). The OCOG retracker, in comparison, is an empirical threshold retracker that relies on shape of the overall width of the waveform to locate the significant wave surface (Ferraro & Swift, 1995), (Tourian et al., 2012).

70



75

80

85

Figure 1: Idealized CryoSat-2 radar waveform (Modified from Simonsen, S. B., & Sorensen, L. S. (2017)). The Leading Edge Width (LeW) is defined as the time or distance it takes for the returning radar waveform to reach peak amplitude from baseline, and the Leading Edge Slope (LeS) is defined as the slope of the waveform during the bins corresponding to the LeW. LeW and LeS have an inverse relationship when the waveform's amplitude remain constant. The UCL-Land Ice (ULI) Retracker models the location of the significant surface height based on the LeS (Schlembach et al., 2020). The OCOG retracker, in comparison, relies on shape of the overall width of the waveform to locate the significant wave surface (Ferraro & Swift, 1995), (Tourian et al., 2012).



90

While in many cases the choice of retracker is inconsequential, UCL-Land Ice's dependence on LeW, which itself can change based on the surface conditions of the targeted surface (Ashcraft & Long, 2005; Legrésy & Rémy, 1997; Nghiem et al., 2001; Nilsson et al., 2015; Simonsen & Sørensen, 2017), may cause inconsistencies if applied uniformly across the GrIS where surface conditions differ across glacial regimes (Benson, 1996; Nghiem et al., 2001, 2012; Polashenski et al., 2014; Rizzoli et al., 2017).

It has been shown, for instance, that the 2012 Melting Event created a Level 2 elevation bias of 89 ± 49 cm at the North Greenland Eemian Drilling Project (NEEM) by artificially decreasing the surrounding waveform's LeW and radar penetration depth in the creation of a more specular melt layer (Nilsson et al. 2015). Since the OCOG Retracker empirically fits a rectangle across the waveform to estimate the amplitude (Ferraro & Swift, 1995) (Tourian et al., 2012) and is not as dependent on LeS as in the ULI retracker, this paper hypothesizes that it should generate a truer elevation trend regardless of shallow subsurface changes such as superficial melting.

105 3. Methodology

We created a framework to calculate and evaluate Level 1B Baseline D LeW and Level 2 elevation time series at any given location on the GrIS within CryoSat-2's Low Resolution Mode (LRM) zone (Ronan et al., 2024). This study in particular focuses on NEEM and Summit Station in the dry-snow zone and Raven Camp in the percolation zone (Benson, 1996; Nghiem et al., 2001, 2012; Polashenski et al., 2014; Rizzoli et al., 2017) (Figure 2). The framework begins by ingesting Level 1B waveforms that were collected within a 20 km radius of NEEM, Summit Station, or Raven Camp, assuming homogeneity within the shallow subsurface across a 125.6 km^2 area (Ronan et al., 2024). Atypical 1B waveforms lacking a characteristic rise to a distinct peak are filtered out, and we calculate the LeW of those remaining. We then produced a time series of one-week average LeW from 2010 to 2021 (Ronan et al., 2024).

115 The framework generates an elevation plane of best-fit from a monthly aggregation of Level 2 elevations within the 125.6 km^2 area, and evaluates the plane at the study location. Level 2 elevations are aggregated monthly as there are not enough collections weekly for a robust multiple regression (Ronan et al., 2024).

120

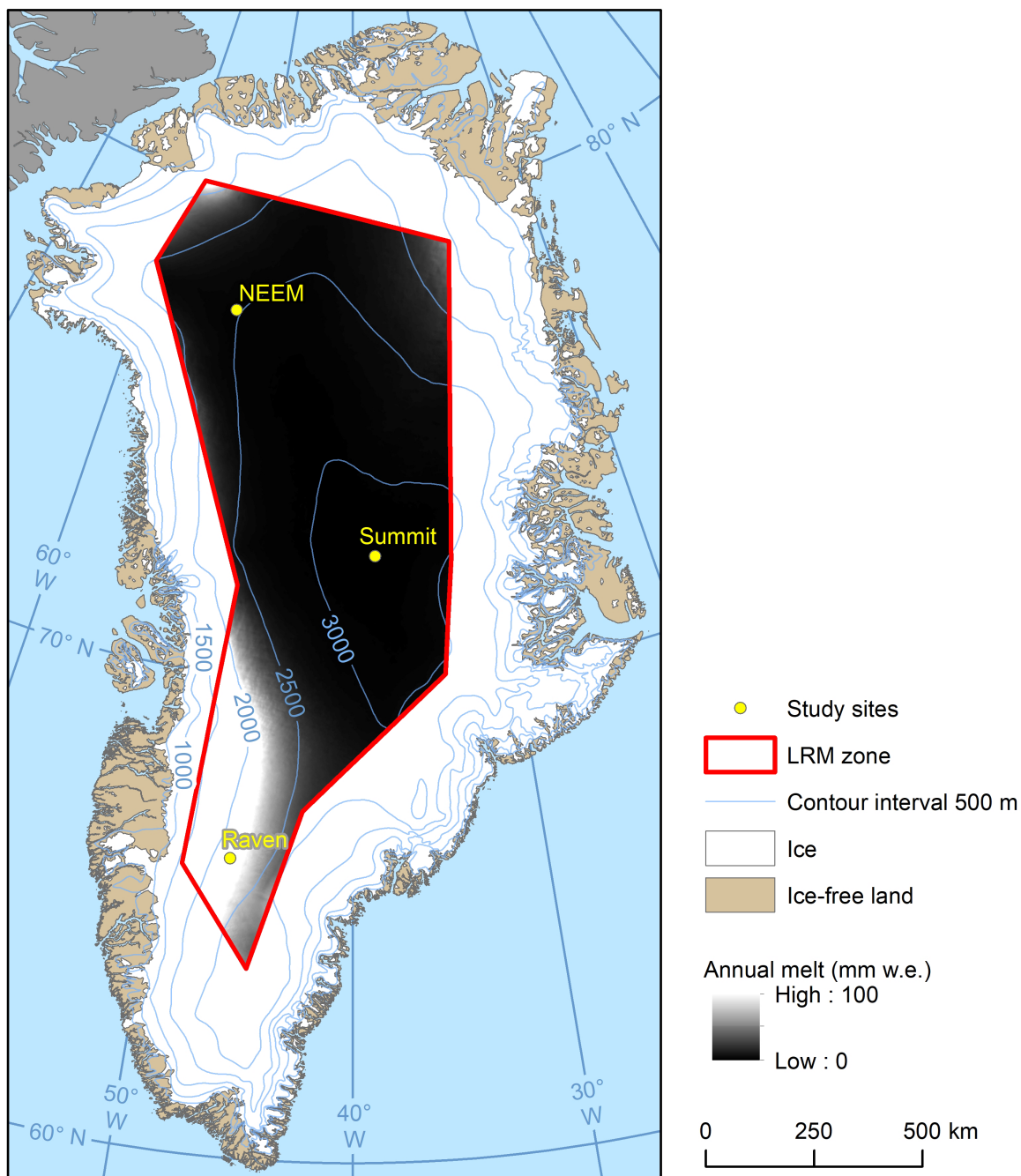




Figure 2: Study sites, elevation (Howat et al., 2015) and mean annual snow melt (Noël et al., 2019) within the LRM Boundary. Raven experiences three orders of magnitude more melt than Summit and two orders of magnitude more melt than NEEM (Noël et al., 2019). Mean annual snow melt is derived from 1958 to 2019 RACMO2.3p2 time series (Noël et al., 2019).

130

The aggregated time series for both Level 1B LeW and Level 2 elevations are analyzed using the Bayesian Estimator for Abrupt Seasonality and Trend (BEAST) algorithm (Zhao et al. 2019), using a 1/8th year interval to derive trends within the clustered time series (Ronan et al., 2024). One outlier cluster was removed from each site's elevation time series (2010-09-13 at Summit Station and 2021-08-24 at Raven Camp). Such clusters were removed for containing elevations greater or less than six standard deviations from the mean of the remaining clusters in the time series. The resulting trends are used to characterize and analyse Level 1B LeW and Level 2 elevation values.

135

140

To account for the difference in aggregation period and allow for separate correlation analysis, Level 1 LeW values are finally interpolated in time to the same dates as Level 2 Elevations (Ronan et al., 2024).

4. Results

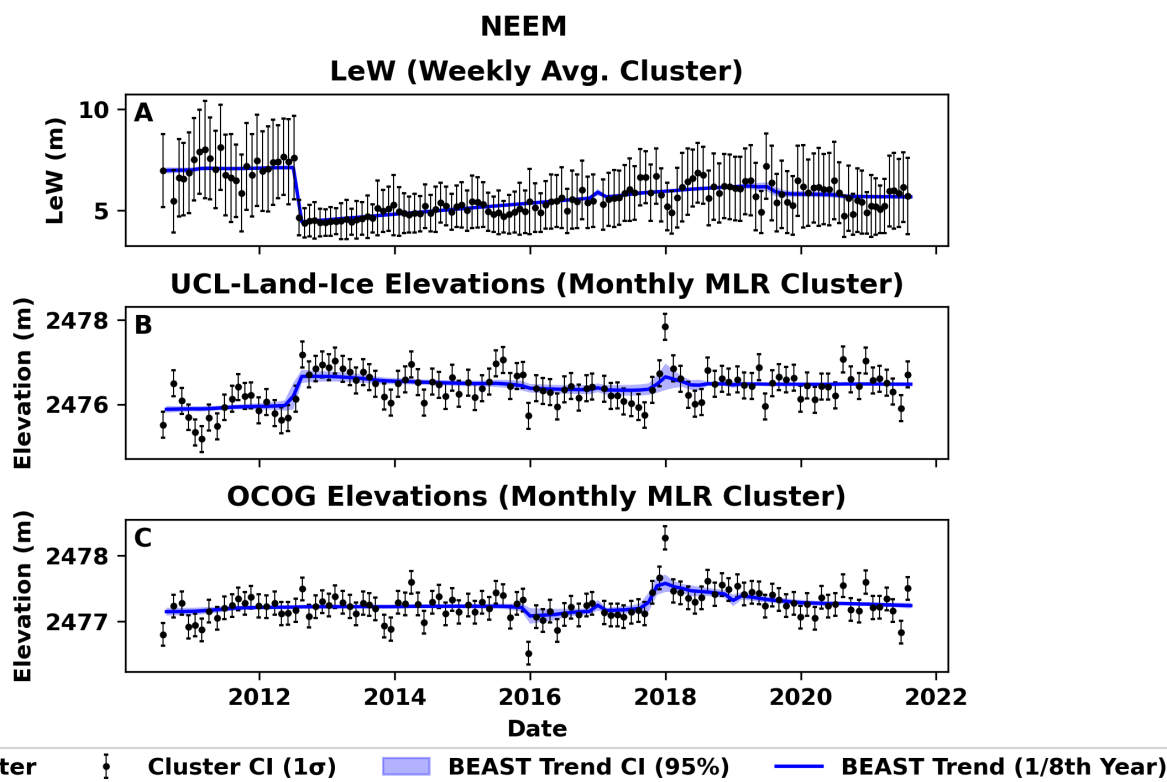
4.1. NEEM

LeW at NEEM increases negligibly from 2010.62 to 2012.5 by 1.99% (6.97 m to 7.12 m) (Figure 3A). From 2012.5 to 2012.62, the LeW abruptly decreased by 46.6% to 4.43 m, and then steadily increased back to 6.20 m (33.4%) and slightly decreases to 5.67 m (-9%) in 2012.62 (Figure 3A). The LeW at NEEM is inversely related to ULI retracked Level 2 elevations (TTT, $\alpha = 0.05$, $r = -0.53$, $p < 0.0001$), and not significantly correlated to the OCOG retracked Level 2 elevations (TTT, $\alpha = 0.05$, $r = 0.03$, $p = 0.81084$). It is noted that the elevation derived from the OCOG retracker at NEEM is on average ~1 m higher than corresponding elevations from the ULI retracker (Figure 3B,3C).

150

155

160



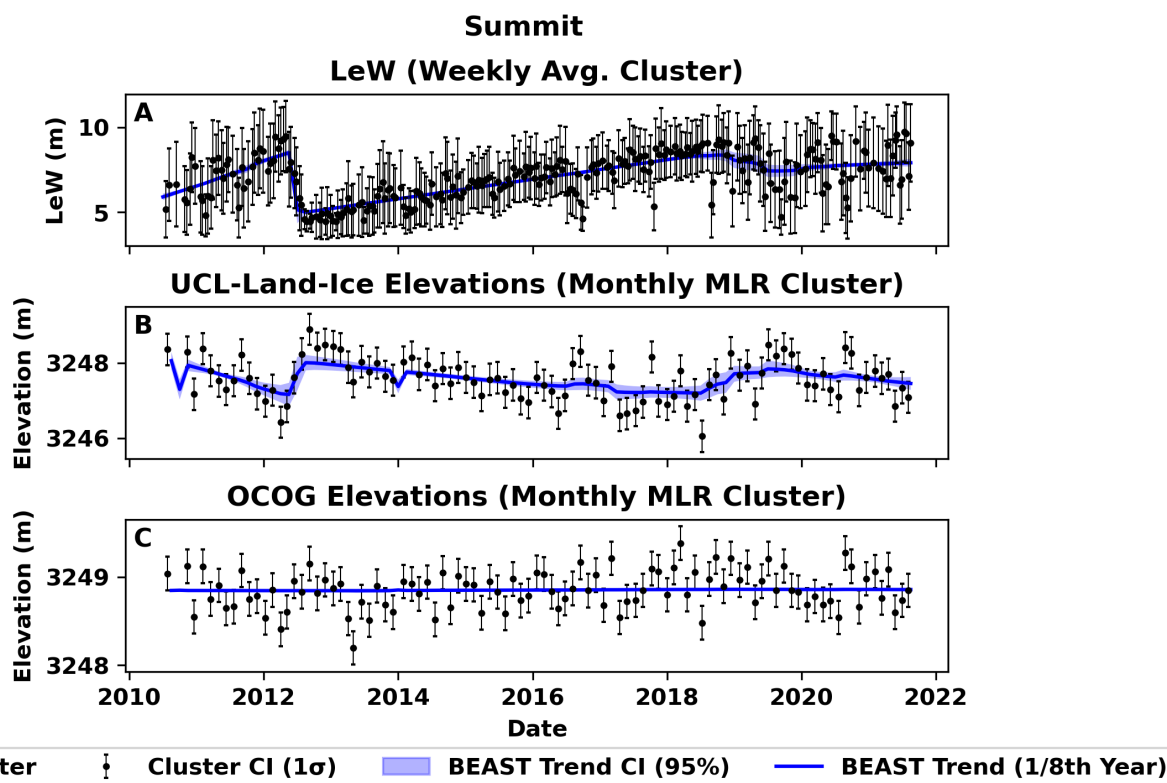
165 Figure 3: NEEM OCOG, UCL-Land Ice Level 2 retracked elevations, and Level 1B LeW. The LeW at NEEM is inversely
 166 related to ULI retracked Level 2 elevations (TTT, $\alpha=0.05$, $r = -0.53$, $p < 0.0001$), and not significantly correlated to the OCOG
 167 retracked Level 2 elevations (TTT, $\alpha=0.05$, $r = 0.03$, $p = 0.81084$). OCOG derived elevations are on average ~1 m higher than
 168 corresponding elevations from the ULI retracker.

170 **4.2. Summit Station**

171 ULI retracker derived elevation trends contain an abrupt increase in July of 2012, followed by a linear decrease in elevation
 172 until ~2018. LeW at Summit increased from 2010.5 to 2012.38 by 36.1% (5.91 m to 8.52 m) (Figure 4A). From 2012.38 to
 173 2012.5, the LeW abruptly decreased by 49.2% to 5.15 m, and then steadily increased to 8.36 m in 2018.99 (Figure 4A). The
 174 LeW ultimately decreased down to 7.22 m in 2019.58 (-15.8%) and recovered back to 7.92 m in 2021.62 (Figure 4A). The
 175 LeW at Summit Station are inversely related to ULI retracked Level 2 elevations (TTT, $\alpha = 0.05$, $r = -0.71$ $p < 0.0001$), and
 176 not significantly correlated to the OCOG retracked Level 2 elevations (TTT, $\alpha = 0.05$, $r = -0.06$, $p = 0.59046$). It is noted
 177 that the elevation derived from the OCOG retracker at Summit Station is on average ~2 m higher than corresponding
 178 elevations from the ULI retracker (Figure 4B, 4C).



180



185 Figure 4: Summit Station OCOG, UCL-Land Ice Level 2 retracked elevations, and Level 1B LeW. The LeW at Summit Station are inversely related to ULI retracked Level 2 elevations (TTT, $\alpha=0.05$, $r = -0.71$ $p < 0.0001$), and not significantly correlated to the OCOG retracked Level 2 elevations (TTT, $\alpha=0.05$, $r = -0.06$, $p = 0.59046$). OCOG derived elevations are on average ~ 2 m higher than corresponding elevations from the ULI retracker.

190 **4.3. Raven Camp**

Unlike NEEM and Summit Station, where there are significant changes in LeW over time (Figure 3A, 4A), the LeW time series at Raven Camp remains constant (Figure 5a). We note that the average LeW at Raven is a full 2 m wider than the largest LeW cluster at Summit (Figure 5C, 5C) (see Discussion for more information). In addition, the LeW time series from Summit Station and NEEM shows a single large and abrupt LeW decrease during the July 2012 melt event (Figure 5A), but 195 no such abrupt change is found in the corresponding LeW time series at Raven Camp. Finally, the elevation estimates from the two retrackerers at Raven camp follow a different pattern than at Summit Station: the variability of elevations derived from



the Land-Ice Retracker is comparable to that of OCOG, and their means are comparable to each other (Figure 5B, 5C). Unlike at Summit Station, the ULI Retracker shows no significant trends during the study period (Figure 5B) or noticeable bias associated with the LeW (TTT, $\alpha = 0.05$, $r = -0.02$ $p = 0.82634$). The OCOG (Figure 5C) behaves the same as in Summit Station, with no noticeable bias associated with the LeW (TTT, $\alpha = 0.05$, $r = -0.071$ $p = 0.48564$).

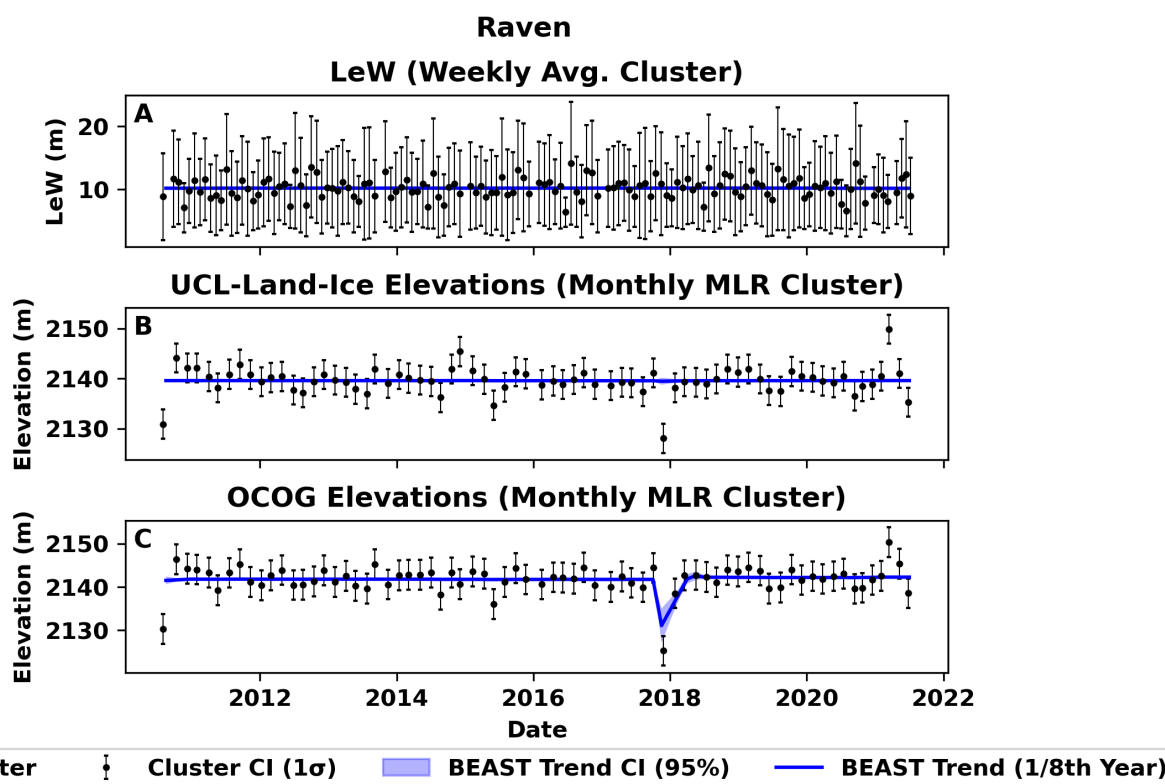


Figure 5: Raven Camp OCOG, UCL-Land Ice Level 2 retracked elevations, and Level 1B LeW. The ULI retracker shows no significant trends during the study period (Figure 4C) or noticeable bias associated with the LeW (TTT, $\alpha=0.05$, $r = -0.02$ $p = 0.82634$). OCOG derived elevations have no noticeable bias associated with the LeW (TTT, $\alpha=0.05$, $r = -0.071$ $p = 0.48564$).

5. Discussion

This study asserts that changes in dry snow zone Level 2 ULI elevations are artifacts of a changing LeW, which in turn are caused by inter and intra seasonal changes in the shallow subsurface. Previous research has demonstrated that when corrected for downslope advection and seasonal variations, the surface elevation at Summit Station is increasing by 0.019 ma^{-1} ($p < 0.0001$, ICESAT-2 Track 412) from at least 2008 to 2018 and is mostly dominated by snow accumulation (Hawley et al., 2020). Given this near-constant trend at Summit Station and concurrence with Nilsson (2015), the ~2 m elevation variation calculated in this study using the ULI elevations at Summit Station and NEEM are unlikely to represent actual elevation change



and is likely an artifact of the waveform's changing LeW. Laser altimetry measurements further corroborate this conclusion
215 as they indicate that the range of surface elevation change within the time frame is one order of magnitude smaller than the
elevation changes indicated by the ULI retracker (Kuipers Munneke et al., 2015). Unlike OCOG derived elevations, which
remain statistically uncorrelated with LeW at NEEM and Summit Station, ULI derived elevations are found to have an inverse
relationship with LeW. Such a relationship can be explained through the inner mechanics of the ULI retracker itself; a
decreased LeW will result in an increased LeS and decreased noise floor, which, when ingested into the Brown – Hayne Model,
220 will find a retracked point in the waveform earlier, which ultimately decreases the calculated time-of-flight of the radar signal
and results in an artificially high surface elevation.

Given the OCOG-derived elevations are ~1m higher than in the ULI algorithm at NEEM and Summit, we assess that the
OCOG behaves as a low-threshold retracker. The OCOG algorithm places the retracked points earlier in the waveform which
225 results in a decreased time-of-flight of the radar signal. As such, OCOG derived elevations escape most artifacts from a
changing LeW that hinder the ULI retracker.

Consistent with Nilsson (2015), we also note significant drops in LeW at NEEM (-46.6%) and Summit Station (-49.2%)
corresponding to the July 2012 Melting Event. We assert that an influx of refrozen meltwater during the 2012 Melting Event
230 on the surface and in the immediate shallow subsurface resulted in a more specular surface and reduction in radar waveform
penetration depth (Nilsson et al., 2015), which significantly increased the surface to volume scattering ratio. Such a dramatic
increase in this ratio results in a sharp decrease in a waveform's LeW. As the melting event subsides and more climatologically
average weather conditions return, the LeW increases as the melt layer is buried and the surface to volume scattering ratio
moves back towards pre-melt values. We see that the LeW at Summit has a higher recovery rate than NEEM, which can be
235 explained by Summit's higher average snow accumulation rates (Noël et al., 2019).

This study also notes a second abrupt decrease in LeW at Summit in Winter 2019 and NEEM in Winter 2020, with no reported
melting event. This may be due to a period of elevated surface wind speeds that, through wind packing, created wind slabs and
crusts (Sommer et al., 2018; Sommer, 2018) and/or removed an upper layer of the loosely layered snowpack. Wind slabs and
240 crusts would result in a decreased LeW through the same mechanism as the melting crust generated from the 2012 Melting
Event. We also note that Summit's LeW is rising at the beginning of the dataset up until the 2012 Melting Event (Figure 4A);
it is possible that there was another melting or wind event pre-2010 from which the LeW is recovering. More research is
needed to investigate the impacts of wind events on the LeW, and to determine the cause of the increasing LeW up until July
2012.

245

Whereas NEEM and Summit Station within the dry snow zone experience shallow subsurface changes resulting in LeW
changes and therefore changes in ULI-derived elevations, no such processes are observed at Raven Camp. Raven experiences



three orders of magnitude more melt than at Summit and two orders of magnitude more melt per year than at NEEM (Noël et al., 2019), and as such, Raven’s shallow subsurface contains vastly more melt layers. We assess that these melt layers keep
250 Raven’s LeW high (~2 m higher in Raven than in NEEM or Summit) through the decrease in penetration depth, and keep the volume to surface scattering ratio low. Such a low ratio suppresses the LeW signal from snow accumulation and minimizes the effect of any high-profile melting crust, and perhaps wind slabs and crusts.

6. Conclusion

255 We analyzed ten-year trends in Level 2 OCOG and UCI retracked GrIS surface elevations, as well as Level 1B LeW from 2010 to 2021. We assess that abrupt 1st order LeW changes within the dry snow zone are a function of large-scale melting events and perhaps wind packing events, whereas 2nd order trends are a function of snowpack recovery. We provide supporting evidence to the assertion of Nilsson et al. (2015) that climatological events impact elevations derived from CryoSAT-2’s SIRAL instrument. We find that the ULI retracker becomes biased within the dry snow zone during periods of intense melt,
260 changing snowpack, and potentially wind events. This is apparent in changes in Level 1B LeW which result in a changing position of the retracked point in the Brown-Hayne Model.

The results from this study indicate that future satellite radar altimeters covering the GrIS dry snow zone must take into consideration climatologically significant events, such as melting events and potentially high-speed wind events and snow
265 accumulation patterns, when analyzing elevations derived from model retracking algorithms.

7. References

- Ashcraft, I. S., & Long, D. G. (2005). Observation and characterization of radar backscatter over Greenland. *IEEE Transactions on Geoscience and Remote Sensing*, 43(2), 225–237. <https://doi.org/10.1109/TGRS.2004.841484>
- 270 Benson, C. S. (1996). *Stratigraphic Studies in the Snow and Firm of the Greenland Ice Sheet*. Snow Ice and Permafrost Research Establishment, Corps of Engineers, U.S. Army. <https://hdl.handle.net/11681/2730>
- Cuffey, K. M., & Marshall, S. J. (2000). Substantial contribution to sea-level rise during the last interglacial from the Greenland ice sheet. *Nature* 2000 404:6778, 404(6778), 591–594. <https://doi.org/10.1038/35007053>
- 275 European Space Agency. (2010). *CryoSat-2 Product Handbook: Baseline D 1.1*. [https://earth.esa.int/eogateway/documents/20142/37627/CryoSat-Baseline-D-Product- Handbook.pdf](https://earth.esa.int/eogateway/documents/20142/37627/CryoSat-Baseline-D-Product-Handbook.pdf) (accessed April 11, 2023)
- Fyke, J. G., Vizcaíno, M., Lipscomb, W., & Price, S. (2014). Future climate warming increases Greenland ice sheet surface mass balance variability. *Geophysical Research Letters*, 41(2), 470–475. <https://doi.org/10.1002/2013GL058172>
- 280 Hawley, R. L., Neumann, T. A., Stevens, C. M., Brunt, K. M., & Sutterley, T. C. (2020). Greenland Ice Sheet Elevation Change: Direct Observation of Process and Attribution at Summit. *Geophysical Research Letters*, 47(22), e2020GL088864. <https://doi.org/10.1029/2020GL088864>



- 285 Howat, I. M. (2022). Temporal variability in snow accumulation and density at Summit Camp, Greenland ice sheet. *Journal of Glaciology*, 68(272), 1076–1084. <https://doi.org/10.1017/JOG.2022.21>
- 290 Kuipers Munneke, P., Ligtenberg, S. R. M., Noël, B. P. Y., Howat, I. M., Box, J. E., Mosley-Thompson, E., McConnell, J. R., Steffen, K., Harper, J. T., Das, S. B., & Van Den Broeke, M. R. (2015). Elevation change of the Greenland Ice Sheet due to surface mass balance and firn processes, 1960–2014. *Cryosphere*, 9(6), 2009–2025. <https://doi.org/10.5194/TC-9-2009-2015>
- Legresy, B., & Remy, F. (1997). Altimetric observations of surface characteristics of the Antarctic ice sheet. *Journal of Glaciology*, 43(144), 265–275. <https://doi.org/10.3189/S002214300000321X>
- 295 Neumann, T. A., Martino, A. J., Markus, T., Bae, S., Bock, M. R., Brenner, A. C., Brunt, K. M., Cavanaugh, J., Fernandes, S. T., Hancock, D. W., Harbeck, K., Lee, J., Kurtz, N. T., Luers, P. J., Luthcke, S. B., Magruder, L., Pennington, T. A., Ramos-Izquierdo, L., Rebold, T., ... Thomas, T. C. (2019). The Ice, Cloud, and Land Elevation Satellite – 2 mission: A global geolocated photon product derived from the Advanced Topographic Laser Altimeter System. *Remote Sensing of Environment*, 233, 111325. <https://doi.org/10.1016/J.RSE.2019.111325>
- 300 Nghiem, S. V., Hall, D. K., Mote, T. L., Tedesco, M., Albert, M. R., Keegan, K., Shuman, C. A., DiGirolamo, N. E., & Neumann, G. (2012). The extreme melt across the Greenland ice sheet in 2012. *Geophysical Research Letters*, 39(20). <https://doi.org/10.1029/2012GL053611>
- 305 Nghiem, S. v., Steffen, K., Kwok, R., & Tsai, W. Y. (2001). Detection of snowmelt regions on the Greenland ice sheet using diurnal backscatter change. *Journal of Glaciology*, 47(159), 539–547. <https://doi.org/10.3189/172756501781831738>
- Nilsson, J., Vallelonga, P., Simonsen, S. B., Sørensen, L. S., Forsberg, R., Dahl-Jensen, D., Hirabayashi, M., Goto-Azuma, K., Hvidberg, C. S., Kjær, H. A., & Satow, K. (2015). Greenland 2012 melt event effects on CryoSat-2 radar altimetry. *Geophysical Research Letters*, 42(10), 3919–3926. <https://doi.org/10.1002/2015GL063296>
- 310 Noël, B., van de Berg, W. J., Lhermitte, S., & van den Broeke, M. R. (2019). Rapid ablation zone expansion amplifies north Greenland mass loss. *Science Advances*, 5(9). https://doi.org/10.1126/SCIADV.AAW0123/SUPPL_FILE/AAW0123_SM.PDF
- 315 Polashenski, C., Courville, Z., Benson, C., Wagner, A., Chen, J., Wong, G., Hawley, R., & Hall, D. (2014). Observations of pronounced Greenland ice sheet firn warming and implications for runoff production. *Geophysical Research Letters*, 41(12), 4238–4246. <https://doi.org/10.1002/2014GL059806>
- 320 Rizzoli, P., Martone, M., Rott, H., & Moreira, A. (2017). Characterization of Snow Facies on the Greenland Ice Sheet Observed by TanDEM-X Interferometric SAR Data. *Remote Sensing* 2017, Vol. 9, Page 315, 9(4), 315. <https://doi.org/10.3390/RS9040315>
- Ronan, A., Hawley, R., & Chipman, J. (2024). Impacts of Differing Melt Regimes on Satellite Radar Waveforms and Elevation Retrievals: Data & Scripts. Zenodo. <https://doi.org/10.5281/zenodo.10969275>
- Sellevoold, R., & Vizcaíno, M. (2020). Global Warming Threshold and Mechanisms for Accelerated Greenland Ice Sheet Surface Mass Loss. *Journal of Advances in Modeling Earth Systems*, 12(9). <https://doi.org/10.1029/2019MS002029>
- 325 Shepherd, A., Ivins, E., Rignot, E., Smith, B., van den Broeke, M., Velicogna, I., Whitehouse, P., Briggs, K., Joughin, I., Krinner, G., Nowicki, S., Payne, T., Scambos, T., Schlegel, N., A. G., Agosta, C., Ahlstrøm, A., Babonis, G., Barletta, V. R.,



... Wuite, J. (2019). Mass balance of the Greenland Ice Sheet from 1992 to 2018. *Nature* 2019 579:7798, 579(7798), 233–239. <https://doi.org/10.1038/s41586-019-1855-2>

330 Simonsen, S. B., & Sorensen, L. S. (2017). Implications of changing scattering properties on Greenland ice sheet volume change from Cryosat-2 altimetry. *Remote Sensing of Environment*, 190, 207–216. <https://doi.org/10.1016/J.RSE.2016.12.012>

Sommer, C. G., Wever, N., Fierz, C., & Lehning, M. (2018). Investigation of a wind-packing event in Queen Maud Land, Antarctica. *Cryosphere*, 12(9), 2923–2939. <https://doi.org/10.5194/TC-12-2923-2018>

Sommer, C. G. (2018). Wind-packing of snow: How do wind crusts form? <https://doi.org/10.5075/EPFL-THESIS-8628>

335 Vermeer, M., Völgyes, D., McMillan, M., & Fantin, D. (2022). CryoSat-2 waveform classification for melt event monitoring. *Proceedings of the Northern Lights Deep Learning Workshop*, 3. <https://doi.org/10.7557/18.6284>

8. Data Availability

The data sets of this study can be located on Github, with the DOI #

10.5281/zenodo.10969275: <https://zenodo.org/records/10969275>

340

9. Code Availability

The resulting data sets of this study can be located on Github, with the DOI #

10.5281/zenodo.10969275: <https://zenodo.org/records/10969275>

345 10. Author contribution

Alexander Ronan, Jonathan Chipman, and Robert Hawley designed the theoretical framework. Alexander Ronan developed and ran the python scripts with assistance from Jonathan Chipman and Robert Hawley.

11. Competing Interest

The authors declare that they have no conflict of interest.

350 12. Funding

Research was funded through NASA- New Hampshire Space Grant (80NSSC20M0051) and Department of Earth Sciences, Dartmouth College, Hanover NH, USA 03755.

13. Acknowledgements

355 We thank the European Space Agency for CryoSat-2 data, which was retrieved from the the FTP server, “science-pds.cryosat.esa.int”